Generation of self-healing beams via four-wave mixing optical mode conversion

Onur Danacı[a], Christian Rios[a], and Ryan T. Glasser[a]

[a]Tulane University, 6400 Freret St., New Orleans, LA, USA

ABSTRACT

We present the experimental conversion of a spatially-Gaussian optical mode into a self-healing, approximate Bessel-Gauss mode by a non-collinear, spatially-multimode four-wave mixing process in warm atomic vapor. In addition to the mode conversion, a second, spatially-separate conjugate beam is created in a non-Gaussian mode that mimics that of the resulting converted probe beam. Additionally, we show that these resulting beams exhibit the ability to partially self-heal their mode profiles after encountering an obstacle in their paths. This multi-spatial-mode nonlinear gain platform may thus be used as a new method for all-optically generating pairs of self-healing beams.

Keywords: Four-wave mixing, nonlinear optics, Bessel-Gauss, self-healing beams

1. INTRODUCTION

Optical beams propagating in non-Gaussian spatial modes have received much attention in recent years. In particular, Bessel-Gauss modes have been shown to exhibit useful properties such as self-healing, limited-diffraction, and extended focal lengths as compared to Gaussian modes.[1–13] Here we demonstrate a new method of generating approximate Bessel-Gauss (BG) modes, namely, non-collinear four-wave mixing (4WM) in warm atomic vapor. As this light-atom process is inherently multi-spatial mode in nature, the presence of a spatially non-Gaussian, strong pump beam can convert a weaker, Gaussian probe beam into a non-Gaussian output beam. Additionally, this process creates a spatially-separate conjugate beam that is in an analogous non-Gaussian mode as the resultant probe beam. Energy conservation and phase-matching conditions result in the well-defined frequencies of the modes, as well as the spatial directions with which they propagate. When the pump is suitably-chosen, these output mode profiles are nearly Bessel-Gaussian, and are shown to exhibit a degree of self-healing as they propagate after encountering an obstruction that blocks more than 70 % of their intensity.

Since the discovery of self-healing, limited-diffraction beams, they have found numerous applications in optical imaging, microsopy, and trapping schemes.[14–24] The self-healing (or self-reconstruction) property of these modes lies in their ability to reconstruct their mode profile after encountering an obstruction that blocks a substantial portion of their intensity. Recently, this property has been exploited to demonstrate the recovery of entanglement after an entangled optical state has been partially obstructed.[25,26]

The four-wave mixing process used here to generate such self-healing optical modes has also been shown to produce highly nonclassical and quantum states of light.[27–31] In particular, photons are created in pairs due to the nonlinear interaction, one of which propagates in the probe mode, and one in a separate conjugate mode. The resulting probe and conjugate beams have been shown to be more strongly correlated than allowed classically, resulting in sub-shot-noise limit noise fluctuations in their intensity-difference. Another interesting aspect of the 4WM process is that when no probe is used to seed the process, the output pairs of photons are entangled in phase-space. These strong nonclassical correlations, combined with the fact that the process inherently supports many spatial modes, has resulted in the demonstration of entangled images and the simultaneous generation of multiple entangled states.[32,33] Additionally, as the process exhibits gain for the probe and conjugate modes, slow- and fast-light effects have been demonstrated when seeding the process with a pulsed probe beam.[34] This dispersive property, again combined with the quantum correlations shared betweeen the probe and conjugate

Further author information: (Send correspondence to R.T.G.)
R.T.G.: E-mail: rglasser@tulane.edu

beams, has allowed for the investigation of the behavior of nonclassical correlations and entanglement in the presence of dispersive media.[35,36]

In this manuscript we show that the same 4WM process may be used to generate non-Gaussian, self-healing optical modes. This includes the conversion of an input Gaussian probe beam to a self-healing beam, as well as the simultaneous generation of a separate conjugate beam in a similar mode that also exhibits the ability to self-reconstruct.

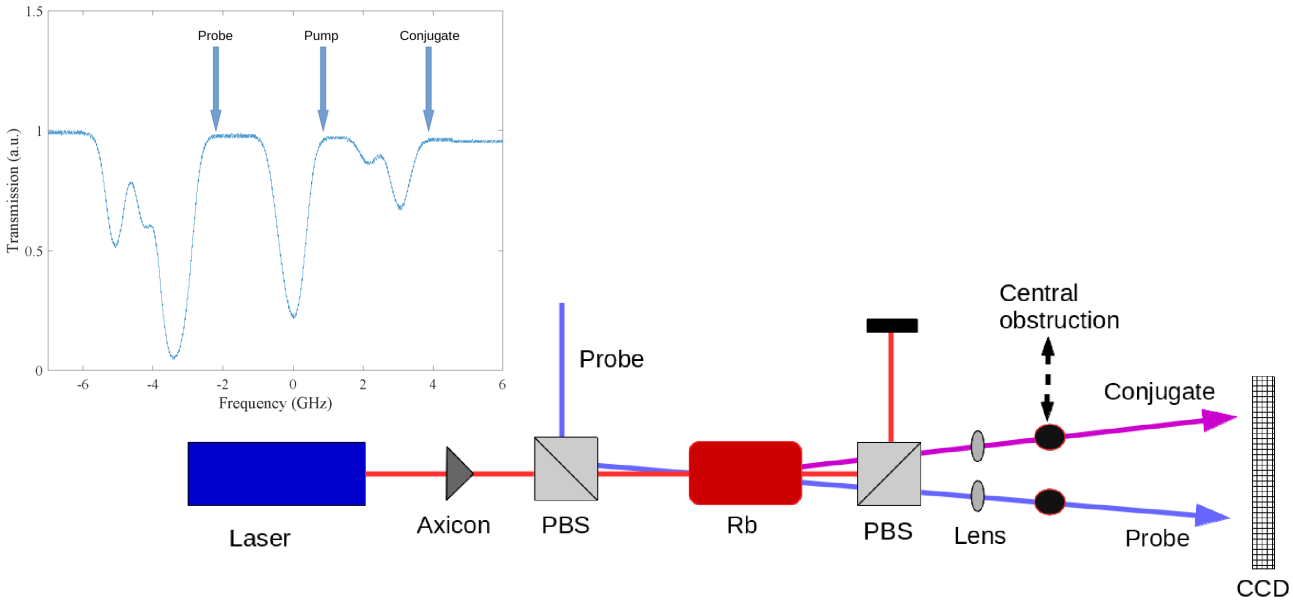

Figure 1: Experimental setup for the generation of self-healing twin beams. Both the pump (red) and probe (blue) beams are derived from the same titanium:sapphire laser. The pump beam passes through an axicon lens, and propagates in an annular, donut-like spatial mode throughout the rubidium vapor interaction region. A small portion of the laser light is picked off before the axicon and double-passed through a high-frequency acousto-optic modulator (not shown) to generate the probe beam that is 3 GHz frequency down-shifted relative to the pump beam. The input probe is in a Gaussian spatial mode that is larger in extent than the annular pump beam. The resulting output probe and conjugate modes are (nearly) collimated with lenses, and are then incident on a CCD array. An obstruction that blocks the central portion of the output beams is inserted when investigating the self-healing properties of the output modes. The transmission profile of a reference, natural abundance rubidium vapor cell, with the relative frequencies of the involved beams, is shown in the top-left.

2. EXPERIMENTAL SETUP

The present experiment involves a third-order nonlinear process in atomic vapor, in which a pair of photons from a strong pump beam are annihilated, and a pair of photons are created in separate optical modes (the probe and conjugate). The pump beam is derived from a continuous-wave titanium:sapphire laser with a power of ∼500 mW, and is passed through an axicon lens. This results in a pump beam that has an annular, donut-like intensity profile (with a null in intensity in the center) with a peak-to-peak diameter of roughly 400 μm throughout the length of the interaction region. The nonlinear medium is an anti-reflection coated rubidium-85 atomic vapor cell that is 1.7 cm long, and is held at a temperature of ∼115 ^{o}C. The pump beam is detuned ∼800 MHz to the blue of the rubidium-85 D1 F = 2 to F = 3 transition. The input probe beam is also derived from the titanium:sapphire laser. A small portion of the laser is split off before the axicon lens and double-passed through a high-frequency (1.5 GHz) acousto-optic modulator. This results in a probe beam that is down-shifted by ∼ 3 GHz relative to the pump beam. The probe and pump beams are linearly polarized, orthogonal to one another. The (spatially) Gaussian probe beam is then combined with the (spatially annular) pump beam on a

polarizing beam splitter and overlapped at roughly an angle of 1^o throughout the length of the rubidium cell, as shown schematically in Figure 1.

Integral to the present experiment is that the input Gaussian (full-width half-maximum of $\sim 1\,\mathrm{mm}$) probe beam is larger in spatial extent than the pump beam. As the process results in the creation of probe (and conjugate) photons only throughout the interaction region (where the beams are spatially-overlapping), only the portions of the probe mode in an annular region defined by the pump beam are amplified. When the gain is large enough (a factor of ~ 30 in the present experiment), the result is a gain-aperturing effect that converts the input probe mode to a non-Gaussian output mode profile that is dependent on the spatial-profile of the pump beam. Additionally, due to phase-matching and energy conservation, the conjugate beam is created in a similar non-Gaussian mode profile, on the opposite spatial side of the pump beam.

3. RESULTS AND DISCUSSION

3.1 Non-Gaussian Modes

The spatial mode profiles of the output probe and conjugate beams are shown in Figure 2. It is directly evident that the mode profiles are non-Gaussian in nature, and exhibit circularly-symmetric oscillations in intensity. The oscillations are more intense along the vertical direction, which is a result of the mismatch in overlap between the pump and probe beam in the vertical and horizontal planes. That is, the pump and probe cross through each other at a small angle throughout the rubidium cell in the horizontal plane. Since there is a null in intensity at the center of the annular pump beam, the probe experiences a smaller effective interaction time along the horizontal plane (again, as it passes through a null-intensity portion of the pump beam). The portions of the probe beam that pass through the top and bottom of the pump beam's annular profile see a longer effective interaction time, as they do not pass through an intensity null. This gives rise to stronger oscillations in the plane orthogonal to that in which the two beams cross one another.

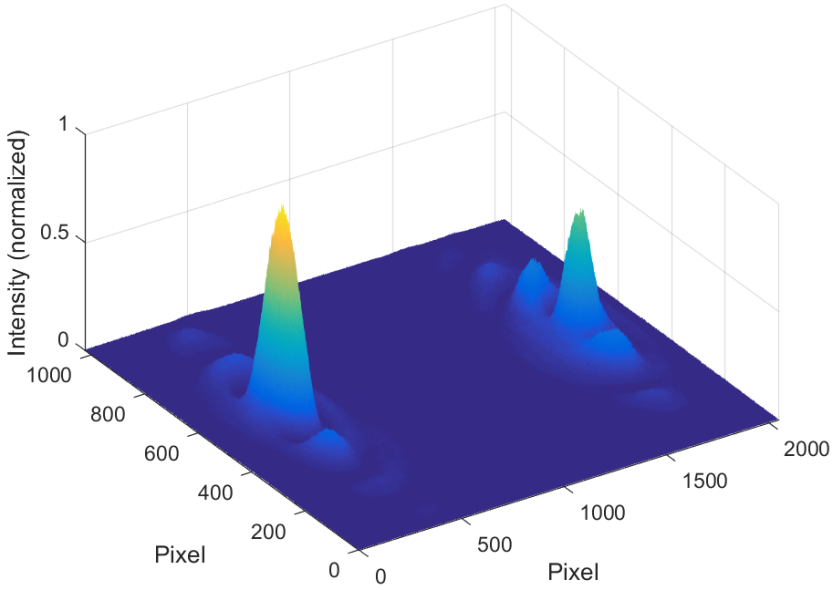

Figure 2: Output probe (right) and generated conjugate (left) mode profiles. Both modes exhibit ring-like intensity oscillations, and are spatially non-Gaussian. The probe beam is slightly weaker than the conjugate beam since it is more on-resonant, and experiences some degree of absorption. The leftover pump beam has been filtered out in post-processing (between the two beams that are shown).

As a check of the non-Gaussianity of the output modes, we first examine the spatial Fourier Transform (FT) of the probe mode. To this end, the output probe beam, after being collimated, is passed through a lens, and a CCD is placed at the focal point. A typical resulting image is shown in Figure 3 (typical conjugate beam FT's are quantitatively very similar).

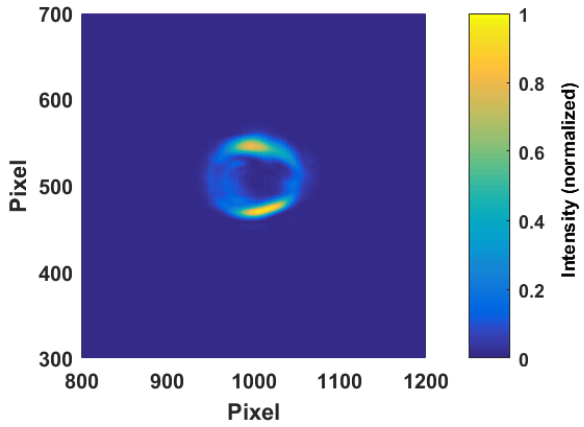

Figure 3: Spatial Fourier Transform of the probe mode shown on the right of Figure 2. This annular profile suggests that the probe mode is both non-Gaussian (as the Fourier Transform of a Gaussian profile is another Gaussian), and that the mode may exhibit self-healing after encountering an obstruction, as discussed in the text.

As seen in Figure 3, the FT of the resulting mode is approximately annular. As the far-field intensity profile of a self-healing Bessel-Gauss mode generated by an axicon lens (or, annular slit followed by a lens) is an annulus, this suggests that the resulting probe and conjugate modes may also exhibit self-healing phenomena, in a manner similar to Bessel-Gauss modes. We note here that the far-field of an ideal Bessel mode is an infinitely-thin annulus.[37] While these ideal Bessel modes exhibit optimal self-healing (while being unphysical since they contain infinite energy, similar to a plane wave), non-ideal Bessel-Gauss modes still exhibit some degree of self-healing after encountering an obstruction.

3.2 Self-Healing Modes

In order to investigate the self-healing capabilities of the modes resulting from the 4WM process, we first collimate the output probe and conjugate beams. After collimation, we then place a rectangular obstruction in the path of the probe (or conjugate) beam and block the central portion of the mode. An image of the probe beam

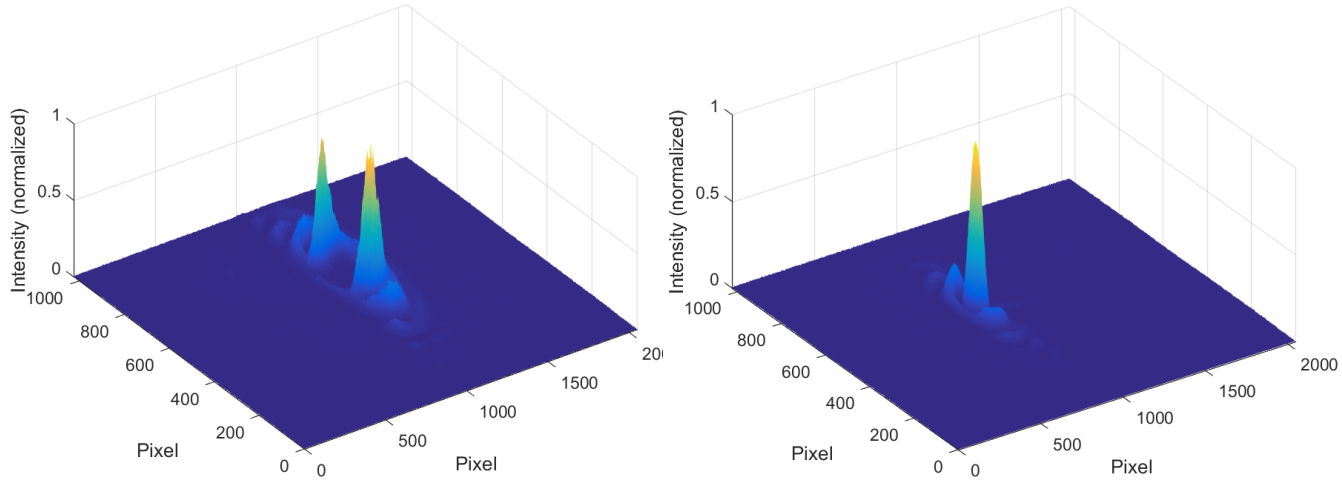

Figure 4: Mode profile of the probe beam immediately after encountering the obstruction in its path (left). Note that the central intensity portion is effectively completely blocked. Reference mode profile of the probe beam (right) at a distance of ~ 1000 mm from the obstruction (no obstruction is present in this reference case). This is to be compared to the reconstructed modes after encountering the obstruction, as shown below in Figure 5.

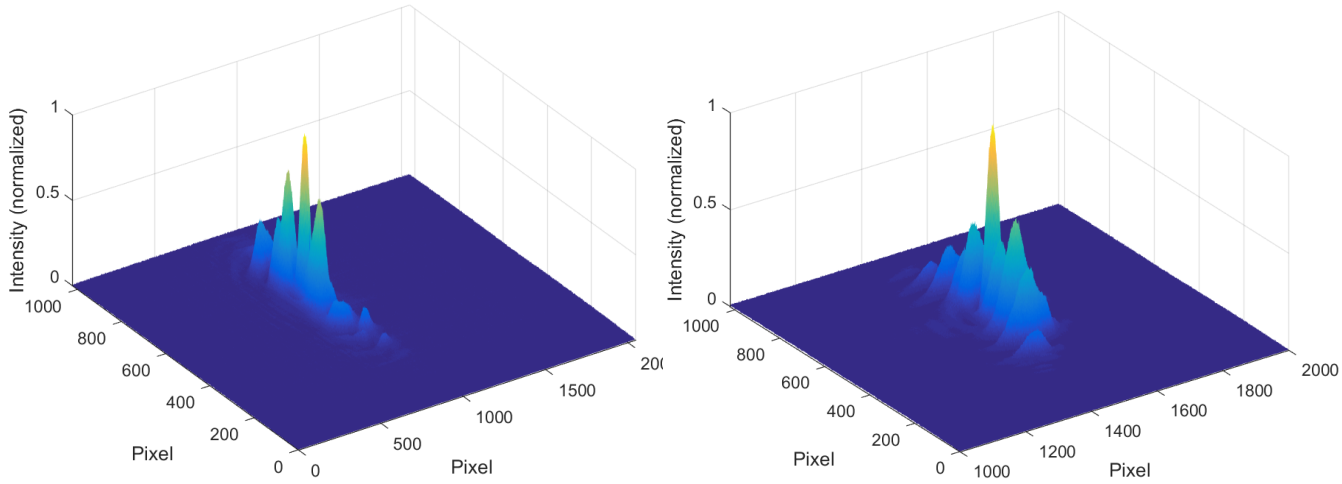

Figure 5: Reconstructed probe mode (left) at a distance of 1000 mm after encountering the obstruction. Reconstructed conjugate mode (right) at a distance of 1000 mm after encountering the obstruction. Note that the central intensity region in both beams that was obstructed has been significantly reconstructed.

immediately after encountering the obstruction is shown on the left side of Figure 4. Note that all of the images shown have their peak intensities normalized, in order to more clearly show the region where the obstruction takes place. A reference image of the probe after propagating ~ 1000 mm from where the obstruction would be placed is shown on the right side of Figure 4 (there is no obstruction present on the right-hand-side of Figure 4).

After encountering the obstruction, the probe (and conjugate) mode then propagates a distance of ~ 1000 mm, after which the central region has been significantly reconstructed. Figure 5 shows the reconstructed profiles of the probe (left) and conjugate (right) after encountering the obstruction at the same distance as the reference, unobstructed mode profile shown on the right of Figure 4. As the modes are clearly not ideal Bessel modes, perfect reconstruction is not to be expected. However, there is a substantial revival of intensity in the central portion of both the reconstructed probe and conjugate modes that was previously obstructed. As seen in Figure 5, the modes have reconstructed such that the peak intensity is again in the central portion of the mode, as in the reference, unobstructed case shown on the right of Figure 4.

In order to directly compare the reference and reconstructed probe beams, we show in Figure 6 vertical (left) and horizontal (right) slices through the center of each beam (each trace is the average of a ten pixel wide slice through the central maximum of the respective modes). The traces are normalized such that their maxima are all one. However, the total intensity in the blocked, reconstructed probe mode is 28.6 % of that in the unblocked, reference probe mode. The full-width half maximum (FWHM) of the central bright spot of the reference, unblocked probe in the vertical direction is $\sim 319\,\mu$m, and that of the reconstructed mode is $\sim 242\,\mu$m. Similarly, the FWHM of the central spot in horizontal direction of the reference probe is $\sim 270\,\mu$m, and $\sim 220\,\mu$m for the reconstructed probe. Additionally, the peak-to-peak diameter of the first ring in vertical direction for the reference probe mode is $\sim 1122\,\mu$m, and $\sim 808\,\mu$m for the reconstructed probe mode. In the horizontal direction, the peak-to-peak diameter of the first-order ring is $\sim 858\,\mu$m for the reference probe mode and $\sim 792\,\mu$m for the reconstructed mode. As seen in Figure 6, the contribution of the first-order ring in the horizontal direction for both the reference and blocked cases is significantly smaller than in the vertical direction. As discussed above, this is due primarily to the asymmetry in effective interaction time in the two planes, due to the annular nature of the pump (which has an intensity null in the central portion). While the obstructed modes are not perfectly reconstructed, it is quite clear that the central region has reconstructed to some degree, and is the most intense portion of the reconstructed modes in all cases.

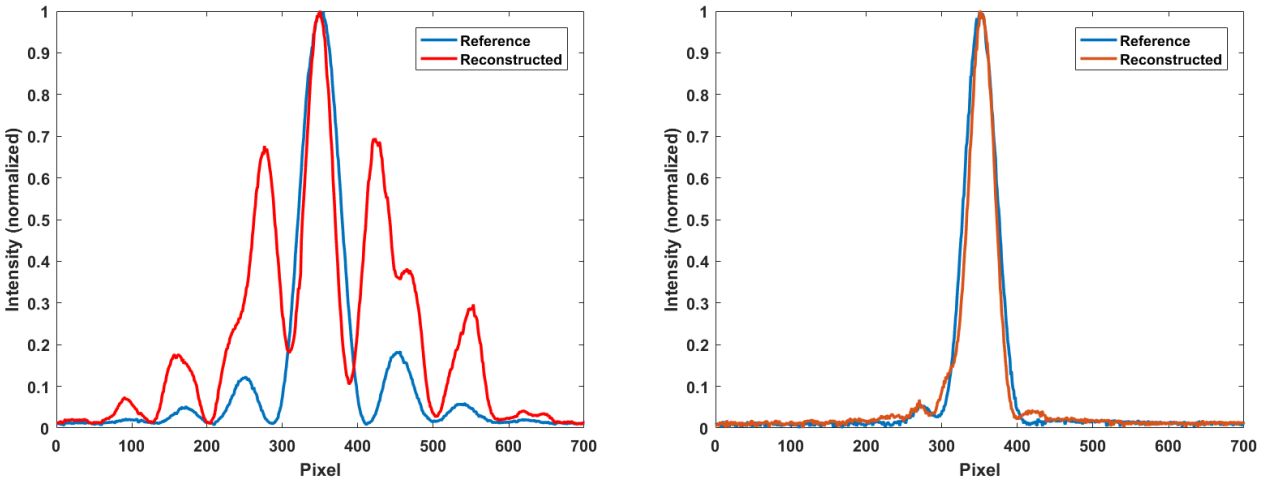

Figure 6: Vertical slices through the reference, unblocked probe (left, blue) and blocked, reconstructed probe (left, red). Horizontal slices through the reference, unblocked probe (right, blue) and blocked, reconstructed probe (right, red). All curves are the average of a ten-pixel wide slice through the central maxima of the reconstructed and reference probe modes.

4. CONCLUSION

In this manuscript we have shown that a spatially-multimode, noncollinear four-wave mixing process in warm atomic vapor may be used to generate self-healing, non-Gaussian optical modes. When the input spatially-Gaussian probe mode is larger in spatial extent than the pump beam, the spatial profile of the pump plays an integral role in the generation of output non-Gaussian probe and conjugate mode profiles. As shown here, when the pump beam exhibits an annular intensity profile, the resulting probe and conjugate modes are converted into approximate Bessel-Gauss modes. In the high-gain regime, this resulting gain-aperturing effect produces amplified (rather than attenuated as in most other means of generating such modes) non-Gaussian modes that exhibit self-healing. We show that when blocking a significant portion of the intensity in the output probe and conjugate modes, their mode profiles tend to self-reconstruct after a finite propagation distance. We anticipate that this four-wave mixing aperturing effect may be used to generate a variety of non-Gaussian optical modes that are applicable to optical communication and imaging schemes.

ACKNOWLEDGMENTS

RTG would like to thank Northrop Grumman - *NG NEXT*, as well as the Louisiana State Board of Regents for support.

REFERENCES

[1] Durnin, J., Miceli, J. J., and Eberly, J. H., "Diffraction-free beams," *Physical Review Letters* **58**, 1499–1501 (Apr. 1987).

[2] Durnin, J., "Exact solutions for nondiffracting beams I The scalar theory," *Journal of the Optical Society of America A* **4**, 651 (Apr. 1987).

[3] Gori, F., Guattari, G., and Padovani, C., "Bessel-Gauss beams," *Optics Communications* **64**, 491–495 (Dec. 1987).

[4] Herman, R. M. and Wiggins, T. A., "Production and uses of diffractionless beams," *Journal of the Optical Society of America A* **8**, 932–942 (June 1991).

[5] McLeod, J. H., "The axicon: A new type of optical element," *Journal of the Optical Society of America (1917-1983)* **44**, 592 (Aug. 1954).

[6] Torres, J. and Torndor, L., [*Twisted Photons: Applications of Light with Orbital Angular Momentum*], Bristol: Wiley-VCH (2011).

[7] Andrews, D. and Babiker, M., [*The Angular Momentum of Light*], Cambridge: Cambridge University Press (2012).

[8] Krenn, M., Robert, Fink, M., Handsteiner, J., Malik, M., Scheidl, T., Ursin, R., and Zeilinger, A., "Communication with spatially modulated light through turbulent air across Vienna," *New Journal of Physics* **16**(11), 113028 (2014).

[9] Wang, J., Yang, J.-Y., Fazal, I. M., Ahmed, N., Yan, Y., Huang, H., Ren, Y., Yue, Y., Dolinar, S., Tur, M., and Willner, A. E., "Terabit free-space data transmission employing orbital angular momentum multiplexing," *Nature Photonics* (2007).

[10] Bozinovic, N., Yue, Y., Ren, Y., Tur, M., Kristensen, P., Huang, H., Willner, A. E., and Ramachandran, S., "Terabit-scale orbital angular momentum mode division multiplexing in fibers," *Science* **340**(6140), 1545–1548 (2013).

[11] Padgett, M., Arlt, J., Simpson, N., and Allen, L., "An experiment to observe the intensity and phase structure of laguerregaussian laser modes," *American Journal of Physics* **64**(1), 77–82 (1996).

[12] Schimpf, D. N., Schulte, J., Putnam, W. P., and Krtner, F. X., "Generalizing higher-order Bessel-Gauss beams: analytical description and demonstration," *Optics Express* **20**, 26852 (Nov. 2012).

[13] McGloin, D. and Dholakia, K., "Bessel beams: diffraction in a new light," *Contemporary Physics* **46**, 15–28 (Jan. 2005).

[14] Sheppard, C., "Use of lenses with annular aperture in scanning optical microscopy," *Optik* **48**(3), 329–334 (1977).

[15] Heckenberg, N. R., McDuff, R., Smith, C. P., Rubinsztein-Dunlop, H., and Wegener, M. J., "Laser beams with phase singularities," *Optical and Quantum Electronics* **24**(9), S951–S962 (1992).

[16] Garcés-Chávez, V., McGloin, D., Melville, H., Sibbett, W., and Dholakai, K., "Simultaneous micromanipulation in multiple planes using a self-reconstructing light beam," *Nature* **419**, 145 (2002).

[17] Mitri, F., "Acoustic radiation force on a sphere in standing and quasi-standing zero-order bessel beam tweezers," *Annals of Physics* **323**(7), 1604 – 1620 (2008).

[18] Duocastella, M. and Arnold, C., "Bessel and annular beams for materials processing," *Laser Photonics Rev.* **6**(5), 607 (2012).

[19] Fahrbach, F., Simon, P., and Rohrbach, A., "Microscopy with self-reconstructing beams," *Nature Phot.* **4**, 780 (2010).

[20] Cotterell, M., Mason, B., Carruthers, A., Walker, J., Orr-Ewing, A., and Reid, J., "Measurements of the evaporation and hygroscopic response of single fine-mode aerosol particles using a bessel beam optical trap," *Phys. Chem. Chem. Phys.* **16**, 2118 (2013).

[21] Curatolo, A., Munro, P., Lorenser, D., Sreekumar, P., Christian Singe, C., Kennedy, B., and Sampson, D., "Quantifying the influence of bessel beams on image quality in optical coherence tomography," *Sci. Rep.* **6**(23483) (2016).

[22] Fahrbach, F. O., Gurchenkov, V., Alessandri, K., Nassoy, P., and Rohrbach, A., "Self-reconstructing sectioned bessel beams offer submicron optical sectioning for large fields of view in light-sheet microscopy," *Opt. Express* **21**, 11425–11440 (May 2013).

[23] Blatter, C., Grajciar, B., Eigenwillig, C. M., Wieser, W., Biedermann, B. R., Huber, R., and Leitgeb, R. A., "Extended focus high-speed swept source oct with self-reconstructive illumination," *Opt. Express* **19**, 12141–12155 (Jun 2011).

[24] Fahrbach, F. and Rohrbach, A., "Propagation stability of self-reconstructing bessel beams enables contrast-enhanced imaging in thick media," *Nature Comm.* **3**(632) (2011).

[25] McLaren, M., Agnew, M., Leach, J., Roux, F. S., Padgett, M. J., Boyd, R. W., and Forbes, A., "Entangled Bessel-Gaussian beams," *Optics Express* **20**, 23589 (Oct. 2012).

[26] McLaren, M., Mhlanga, T., Padgett, M. J., Roux, F. S., and Forbes, A., "Self-healing of quantum entanglement after an obstruction," *Nature Comm.* **5**, 3248 (Feb. 2014).

[27] McCormick, C. F., Boyer, V., Arimondo, E., and Lett, P. D., "Strong relative intensity squeezing by four-wave mixing in rubidium vapor," *Optics Letters* **32**, 178 (Jan. 2007).

[28] McCormick, C. F., Marino, A. M., Boyer, V., and Lett, P. D., "Strong low-frequency quantum correlations from a four-wave-mixing amplifier," *Physical Review A* **78**, 043816 (Oct. 2008).

[29] Pooser, R. C., Marino, A. M., Boyer, V., Jones, K. M., and Lett, P. D., "Low-Noise Amplification of a Continuous-Variable Quantum State," *Physical Review Letters* **103**, 010501 (June 2009).

[30] Marino, A. M., Boyer, V., Pooser, R. C., Lett, P. D., Lemons, K., and Jones, K. M., "Delocalized correlations in twin light beams with orbital angular momentum," *Phys. Rev. Lett.* **101**, 093602 (Aug 2008).

[31] Turnbull, M. T., Petrov, P. G., Embrey, C. S., Marino, A. M., and Boyer, V., "Role of the phase-matching condition in nondegenerate four-wave mixing in hot vapors for the generation of squeezed states of light," *Phys. Rev. A* **88**, 033845 (2013).

[32] Boyer, V., Marino, A. M., and Lett, P. D., "Generation of Spatially Broadband Twin Beams for Quantum Imaging," *Physical Review Letters* **100**, 143601 (Apr. 2008).

[33] Gupta, P., Horrom, T., Anderson, B. E., Glasser, R., and ul D. Lett, P., "Multi-channel entanglement distribution using spatial multiplexing from four- wave mixing in atomic vapor," *Journal of Modern Optics* **63**(3), 185–189 (2016).

[34] Glasser, R. T., Vogl, U., and Lett, P. D., "Stimulated Generation of Superluminal Light Pulses via Four-Wave Mixing," *Physical Review Letters* **108**, 173902 (Apr. 2012).

[35] Vogl, U., Glasser, R. T., Clark, J. B., Glorieux, Q., Li, T., Corzo, N. V., and Lett, P. D., "Advanced quantum noise correlations," *New Journal of Physics* **16**(1), 013011 (2014).

[36] Clark, J. B., Glasser, R. T., Glorieux, Q., Vogl, U., Li, T., Jones, K. M., and Lett, P. D., "Quantum mutual information of an entangled state propagating through a fast-light medium," *Nature Photonics* **8**, 515–519 (July 2014).

[37] Vaity, P. and Rusch, L., "Perfect vortex beam: Fourier transformation of a bessel beam," *Opt. Lett.* **40**, 597–600 (Feb 2015).